PenTag, a Versatile Platform for Covalent Bioconjugation, Purification, and Tagging of Proteins Towards the Development of Novel Biohybrid Material Systems

*Hasti Mohsenin[1,2], Jennifer Pacheco[1,2], Svenja Kemmer[1,3,4], Hanna J. Wagner[1,2], Nico Höfflin[1,2], Toquinha Bergmann[1,3,4], Tim Baumann[1,2], Alexander Ripp[5,6], Nikolaus Jork[1,5,7], Henning J. Jessen[1,5,6], Maja Köhn[1,2], Jens Timmer[1,3,4], Wilfried Weber[1,2,7,8,9]**

Keywords: covalent protein-ligand interaction, protein solubility and purification tags, stimuli-responsive hydrogels, information-processing materials, covalent crosslinking

[1] Signalling Research Centres BIOSS and CIBSS, University of Freiburg, Freiburg, Germany

[2] Faculty of Biology, University of Freiburg, Freiburg, Germany

[3] Institute of Physics, University of Freiburg, Freiburg, Germany

[4] Freiburg Center for Data Analysis and Modelling (FDM), University of Freiburg, Freiburg, Germany

[5] Institute of Organic Chemistry, University of Freiburg, Freiburg, Germany

[6] Cluster of Excellence LivMats, University of Freiburg, Freiburg, Germany

[7] SGBM - Spemann Graduate School of Biology and Medicine, University of Freiburg, Freiburg, Germany

[8] INM – Leibniz Institute for New Materials, Saarbrücken, Germany

[9] Department of Materials Science and Engineering, Saarland University, Saarbrücken, Germany

Abstract

Protein tags play an important role in various chemical biological applications and synthetic biological systems. An ideal protein tag enables labelling of proteins, their monitoring, and detection. Moreover, it forms a stable bond with its specific ligand, which is ideally an available and cheap molecule. Current protein tagging systems are often challenging due to unspecific binding, unstable coupling, or expensive and difficult-to-synthesize ligand molecules. Here, we

present PenTag, an approach for the biorthogonal, and covalent conjugation of a specific protein tag to its ligand for various applications in chemical and synthetic biology. We engineered a new truncated version of penicillin-binding protein 3 (PBP3) and showed that this protein tag can be used for the stable conjugation of proteins to dyes, polymers, or solid supports. We applied PenTag as crosslinking tool for synthesizing stimuli-responsive hydrogels or for the development of a biohybrid material performing computational operations emulating a 4:2 encoder. Based on this broad applicability and the use of a small, cheap and easy-to-functionalize ligand and a stable, soluble recombinant protein, we see PenTag as a versatile alternative to existing protein tags.

Introduction

Protein tags are fundamental modification tools that in recent years have resulted in better understanding of cellular functions, development of novel therapeutics, advanced imaging techniques, and synthesis of protein-based materials[1–6]. Protein tags that bind covalently to their substrates, create a platform for stable and robust anchoring of proteins to small molecules and materials[7–12].

Several techniques have been developed for site-specific conjugation and modification of proteins through covalent binding that have paved their way through various applications in visualizing and manipulating biological processes[13]. Moreover, covalent attachment of chemicals to antibodies or oligonucleotides have resulted in antibody-drug conjugates (ADCs) and antibody-oligonucleotide conjugates (AOCs) as novel therapeutic vehicles for the treatment of various cancers and for non-oncological diseases[14–17]. For example for site-specific protein conjugation, cysteine residues in proteins can be used for bioconjugation of proteins via Thiol-Michael addition reactions of maleimides or vinylsulfones[18–20]. However, if more specific site-selectivity is required, enzymatic labelling techniques, based on, for example *E. coli* biotin ligase BirA, or *Staphylococcus aureus* sortase A (SrtA)-mediated transpeptidation reactions are superior[21,22]. Another technique for site-specific protein labelling uses protein tags that do not require the addition of an additional enzyme that catalyses the coupling reaction[13]. SNAP-, Halo-, and CLIP-Tags are three examples of versatile protein tags that can be used for labelling of proteins for

56 diverse applications such as the specific immobilization and purification of proteins[23–27]. These
57 tags are based on engineered self-modifying enzymes that spontaneously react with O^6-
58 benzylguanine (BG), chloroalkane, and benzylcytosine (BC) derivatives, respectively, leading to a
59 covalent conjugation of the protein to its ligand. These tags are widely used for the spontaneous
60 coupling of proteins to different ligands. However, the required reactive groups are fine
61 chemicals and available in small quantities at rather high prices. Amine-functionalized BG, BC,
62 and HaloTag ligands cost 170, 600, and 140 USD per gram, respectively[28].

63 In addition to mediating site-specific conjugation, an ideal protein tag for synthetic and chemical
64 biology applications enables the detection, visualization, and purification of its fusion partner,
65 confers increased solubility and is able to link the protein of interest to various types of
66 substrates. For some applications, it would be beneficial if the protein tag is small in size and
67 forms a fast and stable bond at a variety of different temperatures and buffer conditions[8,29].
68 Additionally, an ideal ligand would be a simple and cheap chemical that is widely commercially
69 available.

70 ß-lactam antibiotics such as ampicillin have the interesting property that they bind specifically
71 and covalently to penicillin-binding proteins (PBPs). PBPs are transpeptidase enzymes involved in
72 bacterial cell-wall biosynthesis and are the target of ß-lactam antibiotics[30]. Interaction of PBPs
73 with ß-lactam antibiotics starts with the formation of a non-covalent Henri-Michaelis complex
74 and is followed by the attack of the serine residue in the active site of the enzyme to the ß-lactam
75 ring, that results in a covalent acyl-PBP bond[31,32]. In previous works we have applied this specific
76 coupling for the development of microfluidic, point-of-care-suitable assays for electrochemical
77 antibiotics detection in various settings[33–36].

78 Here, we exploit the spontaneous, covalent interaction between ampicillin and PenTag for the
79 development of a protein tag and demonstrate its application in protein immobilization and
80 purification. We use this conjugation technique as a building block towards the design of
81 biohybrid materials performing fundamental computational operations, while showing its
82 biorthogonality to the already existing systems. Besides broad application potential and ease of

83 handling, the bulk availability of ampicillin at very low cost (1.6 USD per gram[28]) is an interesting
84 factor in synthesizing larger quantities of bioconjugates.

85

86 **Results**

87 **Engineered truncated PBP3 binds stably to ß-lactam antibiotics**

88 Large proteins devour more metabolic energy during overexpression in *E. coli* compared to
89 smaller proteins[29]. Further, large proteins represent a less favourable cost-benefit ratio if only
90 one part of the protein structure is needed. However, reducing the size of proteins must be
91 carefully planned and tested to avoid a negative impact on their functionalities. We therefore
92 aimed at the design of a truncated version of PBP3, which is still able to bind to ß-lactam
93 antibiotics. To this aim, we exploited a mutated PBP3[33,37] and the known crystal structure of
94 PBP3[38] to truncate the C-terminal hydrophobic membrane anchor thereby generating a new
95 version of PBP3, termed PBP3-t (Fig. 1a). We produced hexahistidine-functionalized PBP3-t in *E.*
96 *coli*, purified it by immobilized metal affinity chromatography (IMAC), and performed analysis by
97 SDS-PAGE and Coomassie staining. The protein migrated at a position corresponding to 30.2 kDa,
98 which is in agreement with its predicted molecular weight (Fig. S1a).

99 As shown in Figure 1b, derivatives of ß-lactam antibiotics are expected to undergo ring opening
100 when coupled to PenTag. This covalent conjugation could be a useful candidate for protein
101 immobilization and purification, and moreover towards development of smart materials. To
102 evaluate the functionality of PBP3-t compared to PBP3, we separately reacted both proteins with
103 bocillin-FL penicillin, a fluorescent derivative of ß-lactam antibiotics, in a 1:1 protein to bocillin-
104 FL molar ratio at room temperature. To compare the bond between bocillin-FL and both PBP3
105 versions, we measured fluorescence polarization of these conjugates (Fig. 1c). No significant
106 difference could be seen between the polarization of PBP3 and PBP3-t.

107 Furthermore, we tested the stability of the bond between PBP3-t and bocillin-FL over time. We
108 measured the fluorescence polarization of a mixture of PBP3-t and bocillin-FL over 7 days at 4 °C.
109 We did not observe a statistically significant difference in the polarization over time (Fig. 1d).

110 Moreover, we showed that our PenTag-antibiotic complex is most stable at physiological pH
111 (between pH 7.5 and 8.5), which is of high relevance for biorthogonal conjugations (data shown
112 in Supplementary Information, Fig. S1b,c). A major challenge in protein overproduction in *E. coli*
113 is the formation of insoluble aggregates[39]. One promising strategy to overcome this limitation is
114 the fusion to solubilization domains[40], therefore, here we evaluated whether PenTag can be used
115 to increase solubility of an otherwise difficult-to-produce protein and showed its ability to
116 enhance protein solubilization (data shown in Supplementary Information, Fig. S2a).

117 **PenTag as a novel synthesis strategy for stimuli-responsive hydrogels**

118 After validating the interaction between PBP3 versions and ampicillin, we sought to extend this
119 protein-ligand framework in biohybrid hydrogel synthesis. Programmable hydrogels are
120 attractive materials for controlled delivery of biomolecules or as biosensing devices[41–43]. We
121 aimed to develop stimuli-responsive hydrogels benefiting from the covalent bond between the
122 PenTag and its small molecule ligand, ampicillin. For this, we first functionalized four-arm
123 poly(ethylene glycol) succinimidyl carboxymethyl ester (4-arm PEG-SCM) with ampicillin
124 (Supplementary Information Fig. S3), followed by purification via reversed-phased preparative
125 high-performance liquid chromatography (HPLC) to remove unbound ampicillin molecules
126 (Supplementary Information Fig. S4a). For the characterization of the 4-arm PEG-tetra ampicillin,
127 we performed NMR and matrix-assisted laser desorption/ionization time-of-flight (MALDI–ToF)
128 of the purified samples (Fig. S5, and Fig. S4b respectively). The obtained results were in
129 agreement with the expected NMR and MALDI–ToF characterizations.

130 As a crosslinker we designed an mCherry protein which was N- and C-terminally fused to PBP3-t
131 via a linker containing cleavage sites for caspase-3 protease (Casp3). We then mixed 4-arm PEG-
132 ampicillin with the protein crosslinker at a 1 : 4 molar ratio of PenTag : ampicillin. Within 40 h,
133 gelation was observed (Fig. 2a). To test whether a controlled degradation of the hydrogel and
134 release of mCherry is achievable by the stimulus, Casp3, we traced the fluorescence of mCherry
135 in the supernatant after addition of different amounts of Casp3 (Fig. 2b). Whereas no significant
136 mCherry release was observed in the absence of Casp3, increasing protease concentrations
137 correlated with higher mCherry release. These data show that PenTag offers a simple way of

138 synthesizing biohybrid materials e.g., for the controlled, stimulus-dependent release of
139 biomolecular cargos.

140 **PenTag as affinity tag for immobilization of proteins on crosslinked agarose beads**

141 Immobilization of proteins and biomolecules on solid supports enables the development of
142 affinity matrices, micro devices, and bead-based protein assays for multiplexed analytical
143 devices[7,44]. To produce an immobilization matrix to covalently bind PenTag, we functionalized
144 cyanogen bromide (CNBr)-activated crosslinked agarose with ampicillin. CNBr first reacts with
145 hydroxy groups of crosslinked agarose resulting in the formation of reactive cyanate ester groups.
146 The primary amino group of ampicillin subsequently reacts with the cyanate ester, resulting in
147 stable isourea linkages (Fig. 3a)[45]. To test whether ampicillin-functionalized beads can be used
148 for the immobilization and subsequent release of PenTagged proteins, we genetically fused
149 mCherry either to PBP3 or to PBP3-t. In both constructs, a protein linker containing the cleavage
150 site for Casp3 was introduced to allow the release of mCherry from the beads by the addition of
151 Casp3 (Fig. 3b). To measure the binding capacity of the beads, we measured the fluorescence of
152 Casp3-released mCherry and calculated the amount of released protein according to an mCherry
153 standard per ml settled beads (Fig. 3c). The binding capacity of >2 mg protein per ml settled
154 ampicillin-functionalized beads compares favourably to the existing bead functionalization
155 methods of HaloTag and SNAP-Tag with binding capacities of 7 mg and 1 mg protein per ml
156 settled beads, respectively. To assess long-term stability of ampicillin-functionalized beads, the
157 beads were lyophilized and reconstituted in buffer directly after lyophilization or after 18 days
158 storage at 4°C. The binding capacity was assessed as described above and no statistically
159 significant decline was observed in either condition. Moreover, no significant difference was
160 observed between two PenTag versions, meaning that both of them can be used
161 interchangeably. We further assessed PenTag as a purification tag for proteins and compared it
162 to protein purification via IMAC and could show that PenTag can successfully be used as a
163 purification tag as well. Data shown in Supplementary Information Fig. S2b.

164 **Design, characterization, and development of an information processing material system**

165 Biocomputing materials perceive several input stimuli, process those stimuli according to
166 fundamental computational operations and produce a corresponding output. Examples include
167 materials that can count the number of input pulses or that act as signal amplifier via integrated
168 feedback and feedforward loops[11,12,46]. Materials with information-processing capacity enable
169 multiple applications for example in diagnostics or personalized therapy[13]. Among computational
170 operations, the encoder functionality is fundamental in binary data processing with manifold
171 applications e.g. in therapies, medical image analysis, or biosensor fabrication[47,48]. The
172 functionality and the operation characteristics of a 4:2 encoder as well as its implementation by
173 connecting two OR gates is depicted in Fig. 4a,b.

174 To assemble an encoder material framework, we capitalized on our ampicillin-functionalized
175 agarose beads for protein immobilization via PenTag. We first developed two separate agarose-
176 based orthogonal OR gates (Fig. 4c,d), each being responsive to two different proteases and
177 releasing a fluorescent protein, mCherry or GFP, as output. The first OR gate is composed of
178 mCherry genetically fused to PenTag via a linker containing cleavage sites for Casp3 as well as for
179 the tobacco vein mottling virus (TVMV) protease. The fusion protein is covalently coupled to
180 ampicillin-functionalized crosslinked agarose. The addition of either protease is expected to
181 result in the release of mCherry that can be quantified by fluorescence measurement (Fig. 4c).
182 The second OR gate is synthesized from GFP protein genetically fused to HaloTag via a linker
183 containing cleavage sites for tobacco etch virus protease (TEV) and Casp3. This fusion protein is
184 covalently coupled to Halo-ligand-functionalized crosslinked agarose, commercially available
185 HaloLink resin. The addition of TEV OR Casp3 results in the release of GFP that is quantified by
186 fluorescence measurement (Fig. 4d).

187 To characterize each of the OR gates, we first monitored dose-dependent release of mCherry and
188 GFP upon addition of their input proteases (Fig. 4e and Fig. 4f, respectively). We further
189 characterized the cleavage kinetics in response to protease addition. For this, we fixed the
190 protease concentration to the lowest value that resulted in a plateau in the above dose-response
191 measurements (for the mCherry gate: 1.25 µg ml^{-1} for Casp3 and 225 µg ml^{-1} for TVMV; for the
192 GFP gate: 0.625 µg ml^{-1} for Casp3 and 3.125 µg ml^{-1} for TEV). The kinetic data from these
193 experiments were used to parameterize a quantitative mathematical model based on ordinary

194 differential equations (ODEs). In order to identify a parameter combination in which the
195 assembled system would show 4:2 encoder functionality within a desired timeframe (30 min),
196 we simulated the performance of the assembled system as a function of the concentrations of
197 all input proteases (Fig. 4i left) (details of the mathematical model can be found in Supplementary
198 Information, Fig. S6, S7 and Table S2).

199 To confirm the model predictions, an experiment was conducted with the following predicted
200 parameters: final concentrations of 6, 14, and 800 µg ml^{-1} for Casp3, TEV, and TVMV respectively.
201 To assemble the 4:2 encoder, we combined both modules with each other in a single pot in the
202 presence or absence of each of the three input proteases (time-resolved model predictions for
203 the encoder response are shown in Fig. S8a). An output pattern specific for a 4:2 encoder was
204 predicted (Fig. 4i left). This pattern could experimentally be obtained, which demonstrates the
205 functionality of the overall computing network and validates the predictions of the mathematical
206 model (Fig. 4i right, kinetic data in Supplementary Information Fig. S8b).

207 This set-up shows that this novel conjugation platform is biorthogonal to existing protein tags
208 (HaloTag) and can further serve as a robust building block towards the development of
209 information-processing materials.

210

211 **Discussion**

212 We developed a truncated version of PBP3 and demonstrated the covalent binding of both PBP3
213 versions to ampicillin and termed this technology as PenTag. The spontaneous binding of PenTag
214 to its small molecule ligand opened the door for multiple applications in chemical biology and
215 biorthogonal coupling. Protein tags that not only solve purification issues of proteins of interest,
216 but also facilitate protein labelling by organic dyes are extremely beneficial for protein
217 visualization and detection[8]. Moreover, embedding proteins of interest into hydrogels through a
218 covalent protein-ligand interaction can serve as attractive means for the immobilization and
219 controlled delivery of proteins and other molecules[7,13]. Furthermore, such a system that is
220 orthogonal to the existing systems, can extend the library for covalent protein immobilization on
221 materials and enable the development of information-processing materials[9]. A drawback of the

222 already existing systems is the expensive and difficult-to-synthesize small molecules. Here, we
223 benefit from ampicillin as the ligand, a small, available, and cheap molecule that can easily be
224 coupled via its primary amino group to a large variety of N-hydroxy succinimide (NHS)-
225 functionalized commercially available reagents. For example, NHS-functionalized dyes, biotin-
226 labelling reagents, surfaces, polymers, and beads are readily available[34,49–53].

227 In order to introduce a multi-functional protein tag, we first engineered a truncated version of
228 PBP3 with a size of 30.2 kDa, which is 12 kDa smaller than the previous PBP3 version, yet as active
229 as the 42 kDa version. PenTag was shown to enhance the solubility of a fused insoluble protein
230 of interest, to address a common challenge when working with proteins[54]. Our system has shown
231 to be stable at physiological pH values, the environment where most proteins are stable at.
232 Despite the increase in size when fusing PenTag to proteins of interest, this method offers high
233 specificity and does not require addition of an enzyme as for enzyme-based conjugation
234 methods[55–57]. This facilitates downstream processing of functionalized materials.

235 We used PenTag strategy for covalent immobilization of proteins of interest into hydrogels and
236 their controlled release by defined environmental cues. Due to the easy coupling of ampicillin to
237 other molecules, different polymers with various sizes can be functionalized with ampicillin, and
238 thereby desired hydrogels can be tailored depending on the final applications. Here, we chose a
239 4-arm PEG-SCM and functionalized it with ampicillin and could establish covalent crosslinks using
240 PenTag where a controlled release of protein of interest from the hydrogel was achieved by
241 addition of Casp3 protease.

242 Furthermore, we synthesized ampicillin functionalized crosslinked agarose that has applications
243 in various fields, such as protein microdevice assays or for high purity purifications[44,58].
244 Lyophilized ampicillin agarose beads were shown to be stable, which allows the off-the-shelf
245 usage for protein immobilization or capture[59].

246 Signalling and logic circuit designs using proteases have significantly been advanced in the recent
247 years[12,60,61]. Implementation of such circuits onto materials frameworks would add another level
248 of applicability and dimension towards development of powerful information-processing
249 materials[10,11]. Benefiting from various synthetic biological building blocks, we integrated

250 conceptual engineering principles into materials. These materials sense environmental cues as
251 their inputs, can then process information, and finally exhibit a regulated output. In this work,
252 we first assembled simple OR gate material modules using PenTag and compared it to the existing
253 systems. We then did thorough characterization of the both systems by a mathematical model,
254 and finally developed a one-pot combined system that could perform more complicated
255 information processing and produce regulated and clear outputs in a 4:2 encoder design manner.
256 We further validated the predictions of the mathematical model by experimental data.

257 In summary, we introduced a specific and multifunctional protein tag which is highly modular
258 regarding the protein of interest, and even useful when working with insoluble proteins of
259 interest. We showed broad applications for PenTag and specifically demonstrated that hydrogels
260 and other materials systems can be tailored to response to environmental cues, or to perform
261 sensory functions using this strategy.

262 We see PenTag as a versatile, modular tool, orthogonal to existing systems, which is an
263 advantageous candidate for implementation and detection of biological molecules in material
264 frameworks by means of a simple small molecule. Due to its simplicity, cost-efficiency, and high
265 specificity, proteins of interest could covalently and stably be coupled onto different substrates
266 such as hydrogels and other solid supports. We expect that this platform will find broad
267 application not only in chemical and synthetic biology, but also in advanced devices for analytical
268 and diagnostic applications, as controlled drug delivery vehicles, or in tissue engineering and
269 regenerative medicine.

270

271 **Methods**

272 **Cloning of the plasmids**

273 The amino acid sequence of all plasmids and their description are listed in Supplementary
274 Information Table S1. Constructs were cloned by Gibson assembly[62].

275 **Protein expression and purification**

276 For production of all recombinant proteins, plasmids were transformed into *E. coli* BL21 (DE3)
277 pLysS (Invitrogen). Cells were grown at 37 °C while shaking at 150 rpm in LB medium containing
278 100 µg ml^{-1} ampicillin (Carl Roth) and 36 µg ml^{-1} chloramphenicol (Carl Roth). Once an OD_{600} of
279 0.6 was reached, the cultures were induced with 1 mM isopropyl ß-D-1-thiogalactopyranoside
280 (IPTG) and incubated overnight at 18 °C or for 4 h at 30 °C or 37 °C (pKJ57 4 h at 37 °C). Cells were
281 harvested by centrifugation at 6000 x *g* for 10 min and were subsequently resuspended in 35 ml
282 nickel-lysis buffer (50 mM NaH_2PO_4, 300 mM NaCl, 10 mM imidazole, pH 8.0), flash frozen and
283 stored at -80 °C until further use. For lysis, cells were sonicated at 60% amplitude and 0.5 s/ 1 s
284 pulse/ pause intervals with a Sonopuls HD3100 (Bandelin). Crude lysates were centrifuged at
285 30,000 x *g* for 30 min. The protein in the supernatant were purified IMAC, using Ni-NTA Superflow
286 agarose beads (Qiagen) or using ampicillin functionalized agarose. For Ni-NTA purification
287 following the manufacturer's instructions, proteins were loaded onto the already Ni lysis-
288 equilibrated columns, unbound protein was washed away by two wash steps using Ni wash buffer
289 (50 mM NaH_2PO_4, 300 mM NaCl, 20 mM Imidazole, pH 8.0), followed by elution with Ni elution
290 buffer (50 mM NaH_2PO_4, 300 mM NaCl, 250 mM Imidazole, pH 8.0). Eluted proteases were
291 additionally supplemented with 10 mM 2-β-mercaptoethanol (2-ME). All eluted proteins were
292 dialyzed against 5 L 1x PBS using SnakeSkin dialysis tubes with 3.5k molecular weight cut-off
293 (MWCO) (Thermo Fisher Scientific) at 4 °C. Proteins were subsequently analyzed by SDS-PAGE
294 (15% (w/v) gels at 160 V), stained by Coomassie brilliant blue staining, and the concentration of
295 the protein was determined either by SDS-PAGE or by Bradford assay using protein assay dye
296 reagent (Bio-Rad) and bovine serum albumin (Carl Roth) as standard. Measurement was
297 performed in a Multiskan GO spectrophotometer at 575 nm (Thermo Fisher Scientific). In some
298 cases, proteins were concentrated using Spin-X UF 6 columns (Corning Inc., Corning, USA).
299 Purified proteins were supplemented with 15% (v/v) glycerol and stored at -80 °C for further use.

300 For solubility tag experiments, PBP3-t was N-terminally fused to an insoluble construct containing
301 a Pyruvate dehydrogenase complex repressor (PdhR) and an intrinsically disordered protein
302 domain. Protein expression was performed at 18 °C for 16 h.

303 **Fluorescence polarization**

304 To analyze the binding between ampicillin and PenTag, a fluorescent derivate of penicillin,
305 Bocillin-FL (Thermo Fisher Scientific), was incubated with both PBP3 versions in a molar ratio of
306 1:1 at 4 °C, with a final concentration of 50 µM in 1x PBS. Blank samples in the absence of protein
307 were prepared to measure background fluorescence and the fluorescence quenching of the
308 fluorophore when incubated for several days at 4 °C. The mixtures were allowed to reach
309 equilibrium for 1 h at room temperature and then transferred to 4 °C. Fluorescence polarization
310 of 15 µl of the samples in a 384-well plates (Corning 3575) was measured by exciting the samples
311 with polarized light at 485/20 nm and emission at 528/20 nm at a parallel and perpendicular
312 angle for 40 min with an interval of 5 min to make sure the plateau is maintained using a Synergy
313 4 plate reader (BioTek Synergy 4, Vermont, United States). Fluorescence polarization was then
314 calculated using the following equation:

315 $$P = \frac{(F_{\parallel} - F_{\perp})}{(F_{\parallel} + F_{\perp})}$$

316 $F_{\parallel}$ = fluorescence parallel to the excitation plane; $F_{\perp}$ = fluorescence perpendicular to the
317 excitation plane). As negative control the FP of Bocillin-FL alone was measured and its
318 fluorescence quenching over days was used for data normalization.

319

320 **Functionalization of 4-arm PEG with ampicillin**

321 4-arm PEG-NHS, MW 5k (4-arm PEG-SCM, Creative PEG works, Durham, USA) and ampicillin
322 (Roth) were both dissolved in dimethylformamide (DMF) with a concentration of 100 mg ml^{-1} and
323 20 mg ml^{-1} respectively. A 6x molar excess of ampicillin (192 µmol) was mixed with 15 µmol
324 triethylamine (Sigma) prior to being added drop-wise to PEG-SCM (32 µmol). All steps were
325 conducted in an exicator under argon flow. For purification, preparative HPLC (Agilent
326 Technologies 1260 Infinity I/II) was conducted to separate excess ampicillin from PEG-tetra-
327 ampicillin. Briefly, preparative HPLC was employed using a reversed-phase C18 column
328 (Macherey-Nagel VP 250/21 Nucleodur 100-5) with a mobile phase solvent A (Water + 0.05%
329 vol/vol trifluoroacetic acid (TFA)), solvent B (acetonitrile + 0.05% vol/vol TFA). The column was

330 eluted with a gradient of solvent B 10-90% over 20 minutes at a flow rate of 20 ml min^{-1}, and
331 fractions were monitored by UV-absorption at 230 nm.

332 **Characterization of the polymer**

333 Samples of collected fractions of preparative HPLC were monitored by MALDI-ToF mass
334 spectrometry to confirm the right size of the purified samples. For this, samples were dissolved
335 in acetonitrile (HPLC grade). 5 µl of the sample solution was mixed with 5 µl of a saturated
336 solution of α-cyano-4-hydroxycinnamic acid matrix for MALDI-MS (Sigma-Aldrich) in acetonitrile.
337 1.5 µl of the latter mixture was applied to the MALDI target and let dry. Analysis was carried out
338 on a Microflex MALDI mass spectrometer (Bruker) and data was processed via mMass software
339 and GraphPad Prism.

340 For precise characterization of the final product and free ampicillin molecule, ^{1}H NMR spectra
341 were recorded at room temperature on a Bruker Avance Neo (400 MHz). Samples were dissolved
342 in deuterated DMSO or chloroform.

343 Once the fractions were characterized, they were freeze-dried and lyophilized. Samples were
344 subsequently diluted in ddH_2O and stored at -20 °C for further use.

345 **Hydrogel synthesis**

346 For hydrogel synthesis, purified PBP3t-mCherry-PBP3t (pHM528) was concentrated to ~150 mg
347 mL^{-1} by centrifugation using Spin-X UF 20 mL centrifugal concentrators (30 kDa MWCO, Corning
348 Inc., Corning, USA). Hydrogels of 10 µL volume were produced by mixing 14.6 nmol PBP3t-
349 mCherry-PBP3t (pHM528) with PEG-tetra-ampicillin in PBS in a 1:4 PenTag : ampicillin molar ratio.
350 Glass slides were siliconized by Sigmacote (Sigma-Aldrich) according to manufacturer's
351 instructions. Briefly, clean glass slides were immersed in Sigmacote, air-dried under a fume hood,
352 and were subsequently washed with water and let dry. The polymer-protein mixture was spotted
353 on siliconized glass slides and incubated at room temperature for ~40 h under humidifying
354 atmosphere. Afterwards, the hydrogels were transferred to 1 mL 1x PBS and incubated for 6 h to
355 let the hydrogels swell. Swollen hydrogels were subsequently transferred to different
356 experimental set-ups and incubated for 2 h in 200 µL 1x PBS with 10 mM 2-ME and at room

357 temperature on an orbital shaker. Fluorescent measurements of the supernatant were carried
358 out at desired time points at 575/620 nm Ex/Em and the % dissolution was measured by dividing
359 the fluorescent intensity by the maximum mCherry fluorescent intensity upon complete gel
360 dissolution.

361 **Functionalization of CNBr-activated Sepharose 4B beads**

362 Ampicillin-beads were produced by coupling ampicillin to CNBr-activated Sepharose beads (GE
363 Healthcare). Coupling was performed according to manufacturer's instructions. Briefly, 1 g of the
364 lyophilized beads were washed for 30 min with ice cold 1 mM HCl to preserve the activity of the
365 reactive groups. The beads were then equilibrated with coupling buffer (0.1 M $NaHCO_3$, 0.5 M
366 NaCl, pH 8.3) and subsequently 1 ml ampicillin (4.57 mM diluted in water) was added to the
367 beads. The mixture was incubated overnight at 4 °C on a rotary shaker. The next day, excess
368 ampicillin was washed away with coupling buffer. To block any remaining active groups, the
369 beads were slowly agitated for 2 h in blocking buffer (0.1 M Tris-HCl, pH 8.0) followed by four
370 wash cycles with alternating pH buffers (0.1 M acetic acid/sodium acetate with 0.5 M NaCl, pH 4
371 and 0.1 M Tris-HCl with 0.5 M NaCl, pH 8.0). Finally, beads were washed with deionized water
372 (ddH_2O) and transferred to 10 mg mL^{-1} BSA dissolved in water and incubated overnight at 4 °C on
373 a rotary shaker. After coupling, the beads were lyophilized (Christ Alpha 1-4 LSCbasic, Germany)
374 and stored at 4 °C for further use.

375 **Binding capacity and purification tag**

376 For binding capacity tests, 500 µl of the settled ampicillin beads were incubated overnight at 4°C
377 with 4.5 mg of protein PBP3-CCS-mCherry (pHM151) or PenTag-CCS-mCherry (pHM525). On the
378 following day, the beads were washed four times with 1x PBS and the supernatant of the wash
379 fractions was kept for later measurements. To measure the binding capacity, 80 µl of the settled
380 beads bound to the protein were added to 200 µl 1x PBS containing 10 mM 2-ME and 20 µl of
381 Casp3 (0.5 mg ml^{-1}). After incubating for 1 h the relative fluorescence unit (RFU) of the
382 supernatant was measured at 575/620 nm Ex/Em using an Infinite M200 pro micro plate reader
383 (Tecan). The fluorescence was correlated to dilution series of each protein with concentrations

384 between 0 and 1.5 mg ml^{-1} and thereby the binding capacity was reported as mg protein per ml
385 settled beads.

386 **Encoder system**

387 Prior to assembling the encoder system, each OR-gate was established separately. OR gate 1 was
388 prepared by immobilizing PBP3-fused mCherry protein (pHM151) onto ampicillin-functionalized
389 crosslinked material as explained in "binding capacity" section. To characterize this system, a
390 dose-dependent mCherry release was monitored by the addition of different concentrations of
391 TEV (pRK793) and Casp3 (pKJ57) proteases, using 7 µl settled beads per reaction, all reactions in
392 200 µl 1x PBS supplemented with 10 mM 2-ME and Tween-20 and the respective protease
393 concentrations. For time kinetic measurements, a specific concentration for each protease was
394 chosen (1.25 µg ml^{-1} for Casp3 and 225 µg ml^{-1} for TVMV). For each time point, a 200 µl reaction
395 mixtures was prepared. Samples were taken in triplicates and measured at 575/625 nm Ex/Em
396 as explained above. For OR Gate 2, HaloTagged GFP (pHM150) was coupled onto HaloLink™ resin
397 (Promega) following the manufacturer's instructions. Briefly, 500 µl of settled beads were
398 equilibrated with binding buffer (100 mM Tris/HCl, 150 mM NaCl, 0.5% Triton, pH 7.6) and
399 incubated with 3.6 mg GFP protein on a rotary shaker overnight at 4 °C. On the following day,
400 beads were washed 4 times with binding buffer. Conduction of the dose-response and kinetic
401 measurements were similar to the first OR gate. For dose response measurements, the only
402 difference was that 5 µl of settled beads were used for each condition. For time kinetic
403 measurements, 0.625 µg ml^{-1} Casp3 and 3.125 µg ml^{-1} TEV were used. For the encoder system,
404 both proteins were coupled onto their respective material frameworks and the crosslinked
405 materials (5 µl GFP settled beads, and 7 µl mCherry settled beads) were mixed together in 2 ml
406 1x PBS, supplemented with 10 mM 2-ME and final concentrations of 6, 14, and 800 µg ml^{-1} for
407 Casp3, TEV, and TVMV were added respectively. The measured RFU for each gate was normalized
408 to the maximum RFU values after 55 min and values were reported as percentage of released
409 proteins. A time kinetic measurement was performed for the encoder system combination for 55
410 min every 5 min.

411

Code availability

The numerical integration, fitting process and identifiability analysis with the profile likelihood method were performed in R using the freely available software package dMod. Used equations and model details can be found in the Supplementary Information. Source data are provided with this paper.

417 **References**

418 1. Macdonald, J. I., Munch, H. K., Moore, T. & Francis, M. B. One-step site-specific
419 modification of native proteins with 2-pyridinecarboxyaldehydes. *Nat. Chem. Biol.* **11**,
420 326–331 (2015).

421 2. Griffin, B. A., Adams, S. R. & Tsien, R. Y. Specific covalent labeling of recombinant protein
422 molecules inside live cells. *Science (80-.).* **281**, 269–272 (1998).

423 3. Shiraiwa, K., Cheng, R., Nonaka, H., Tamura, T. & Hamachi, I. Chemical Tools for
424 Endogenous Protein Labeling and Profiling. *Cell Chem. Biol.* **27**, 970–985 (2020).

425 4. Backus, K. M. *et al.* Proteome-wide covalent ligand discovery in native biological systems.
426 *Nature* **534**, 570–574 (2016).

427 5. Nomura, D. K., Dix, M. M. & Cravatt, B. F. Activity-based protein profiling for biochemical
428 pathway discovery in cancer. *Nat. Rev. Cancer* **10**, 630–638 (2010).

429 6. Xue, L., Karpenko, I. A., Hiblot, J. & Johnsson, K. Imaging and manipulating proteins in live
430 cells through covalent labeling. *Nat. Chem. Biol.* **11**, 917–923 (2015).

431 7. Gawade, P. M., Shadish, J. A., Badeau, B. A. & DeForest, C. A. Logic-Based Delivery of Site-
432 Specifically Modified Proteins from Environmentally Responsive Hydrogel Biomaterials.
433 *Adv. Mater.* **31**, 1–6 (2019).

434 8. Hoelzel, C. A. & Zhang, X. Visualizing and Manipulating Biological Processes by Using
435 HaloTag and SNAP-Tag Technologies. *ChemBioChem* **21**, 1935–1946 (2020).

436 9. Ikeda, M. *et al.* Installing logic-gate responses to a variety of biological substances in
437 supramolecular hydrogel-enzyme hybrids. *Nat. Chem.* **6**, 511–518 (2014).

438 10. Wagner, H. J. *et al.* Synthetic biology-inspired design of signal-amplifying materials
439 systems. *Mater. Today* (2018).

440 11. Beyer, H. M. *et al.* Synthetic Biology Makes Polymer Materials Count. *Adv. Mater.* **30**, 1–7
441 (2018).

442 12. Wagner, H. J., Kemmer, S., Engesser, R., Timmer, J. & Weber, W. Biofunctionalized
443 Materials Featuring Feedforward and Feedback Circuits Exemplified by the Detection of
444 Botulinum Toxin A. *Adv. Sci.* **6**, (2019).

445 13. Wagner, H. J., Mohsenin, H. & Weber, W. Synthetic Biology-Empowered Hydrogels for
446 Medical Diagnostics BT - Tunable Hydrogels: Smart Materials for Biomedical Applications.
447 in (eds. Lavrentieva, A., Pepelanova, I. & Seliktar, D.) 197–226 (Springer International
448 Publishing, 2021).

449 14. Theocharopoulos, C., Lialios, P. P., Samarkos, M., Gogas, H. & Ziogas, D. C. Antibody-drug
450 conjugates: Functional principles and applications in oncology and beyond. *Vaccines* **9**,
451 (2021).

452 15. Dugal-Tessier, J., Thirumalairajan, S. & Jain, N. Antibody-oligonucleotide conjugates: A
453 twist to antibody-drug conjugates. *J. Clin. Med.* **10**, 1–17 (2021).

454 16. Cao, W. *et al.* Antibody–siRNA conjugates (ARC): Emerging siRNA drug formulation. *Med.*
455 *Drug Discov.* **15**, 100128 (2022).

456 17. Fu, Z., Li, S., Han, S., Shi, C. & Zhang, Y. Antibody drug conjugate: the "biological missile"
457 for targeted cancer therapy. *Signal Transduct. Target. Ther.* **7**, (2022).

458 18. Lyon, R. P. *et al.* Self-hydrolyzing maleimides improve the stability and pharmacological
459 properties of antibody-drug conjugates. *Nat. Biotechnol.* **32**, 1059–1062 (2014).

460 19. Masri, M. S. & Friedman, M. Protein reactions with methyl and ethyl vinyl sulfones. *J.*
461 *Protein Chem.* **7**, 49–54 (1988).

462 20. Nair, D. P. *et al.* The Thiol-Michael addition click reaction: A powerful and widely used tool
463 in materials chemistry. *Chem. Mater.* **26**, 724–744 (2014).

464 21. Chen, I., Howarth, M., Lin, W. & Ting, A. Y. Site-specific labeling of cell surface proteins
465 with biophysical probes using biotin ligase. *Nat. Methods* **2**, 99–104 (2005).

466 22. Voloshchuk, N., Liang, D. & Liang, J. Sortase A Mediated Protein Modifications and Peptide
467 Conjugations. *Curr. Drug Discov. Technol.* **12**, 205–213 (2016).

468 23. Keppler, A. *et al.* A general method for the covalent labeling of fusion proteins with small
469 molecules in vivo. *Nat. Biotechnol.* **21**, 86–89 (2003).

470 24. Los, G. V *et al.* HaloTag: A Novel Protein Labeling Technology for Cell Imaging and Protein
471 Analysis. *ACS Chem. Biol.* **3**, 373–382 (2008).

472 25. Gautier, A. *et al.* An Engineered Protein Tag for Multiprotein Labeling in Living Cells. *Chem.*
473 *Biol.* **15**, 128–136 (2008).

474 26. Liss, V., Barlag, B., Nietschke, M. & Hensel, M. Self-labelling enzymes as universal tags for
475 fluorescence microscopy, super-resolution microscopy and electron microscopy. *Sci. Rep.*
476 **5**, 1–13 (2015).

477 27. Wilhelm, J. *et al.* Kinetic and Structural Characterization of the Self-Labeling Protein Tags
478 HaloTag7, SNAP-tag, and CLIP-tag. *Biochemistry* **60**, 2560–2575 (2021).

479 28. Scifinder. *'Chemical CAS no. search results', Accessed April 12, 2023.* Available at:
480 https://scifinder-n.cas.org/.

481 29. Waugh, D. S. Making the most of affinity tags. *Trends Biotechnol.* **23**, 316–320 (2005).

482 30. Hamed, R. B. *et al.* The enzymes of β-lactam biosynthesis. *Nat. Prod. Rep.* **30**, 21–107
483 (2013).

484 31. Shalaby, M. A. W., Dokla, E. M. E., Serya, R. A. T. & Abouzid, K. A. M. Penicillin binding
485 protein 2a: An overview and a medicinal chemistry perspective. *Eur. J. Med. Chem.* **199**,
486 112312 (2020).

487 32. Proteins, P. Kinetics of b -Lactamases and Penicillin-Binding Proteins 12. 195–214 (2020).

488 33. Bruch, R. *et al.* Clinical on-site monitoring of ß-lactam antibiotics for a personalized
489 antibiotherapy. *Sci. Rep.* **7**, 1–10 (2017).

490 34. Ates, H. C. *et al.* Biosensor-Enabled Multiplexed On-Site Therapeutic Drug Monitoring of
491 Antibiotics. *Adv. Mater.* **34**, (2022).

492 35. Glatz, R. T., Ates, H. C., Mohsenin, H., Weber, W. & Dincer, C. Designing electrochemical
493 microfluidic multiplexed biosensors for on-site applications. *Anal. Bioanal. Chem.* (2022).

494 36. Johnston, M. *et al.* Multiplexed biosensor for point-of-care COVID-19 monitoring: CRISPR-
495 powered unamplified RNA diagnostics and protein-based therapeutic drug management.
496 *Mater. Today* **61**, 129–138 (2022).

497 37. Zhang, J., Wang, Z., Wen, K., Liang, X. & Shen, J. Penicillin-binding protein 3 of
498 Streptococcus pneumoniae and its application in screening of β-lactams in milk. *Anal.*
499 *Biochem.* **442**, 158–165 (2013).

500 38. Morlot, C. *et al.* Crystal structure of a peptidoglycan synthesis regulatory factor (PBP3)
501 from Streptococcus pneumoniae. *J. Biol. Chem.* **280**, 15984–15991 (2005).

502 39. Chayen, N. E. Turning protein crystallisation from an art into a science. *Curr. Opin. Struct.*
503 *Biol.* **14**, 577–583 (2004).

504 40. Ki, M. R. & Pack, S. P. Fusion tags to enhance heterologous protein expression. *Appl.*
505 *Microbiol. Biotechnol.* **104**, 2411–2425 (2020).

506 41. Gübeli, R. J. *et al.* Remote-Controlled Hydrogel Depots for Time-Scheduled Vaccination.
507 5355–5362 (2013).

508 42. Li, J. & Mooney, D. J. Designing hydrogels for controlled drug delivery. *Nat. Rev. Mater.* **1**,
509 16071 (2016).

510 43. Badeau, B. A. & Deforest, C. A. Programming Stimuli-Responsive Behavior into
511 Biomaterials. *Annu. Rev. Biomed. Eng.* **21**, 241–265 (2019).

512 44. Chan, L. *et al.* Covalent attachment of proteins to solid supports and surfaces via sortase-
513 mediated ligation. *PLoS One* **2**, 1–5 (2007).

514 45. Wilchek, M., Oka, T. & Topper, Y. J. Structure of a soluble super active insulin is revealed
515 by the nature of the complex between cyanogen bromide activated Sepharose and amines
516 (N substituted isoureas/N1 N2 disubstituted guanidines/insulin Sepharose/insulin
517 insensitivity/super active peptid. *Proc. Natl. Acad. Sci. U. S. A.* **72**, 1055–1058 (1975).

518 46. Wagner, H. J. *et al.* Synthetic biology-inspired design of signal-amplifying materials
519 systems. *Mater. Today* **22**, 25–34 (2019).

520 47. He, K. *et al.* Transformers in medical image analysis. *Intell. Med.* **3**, 59–78 (2023).

521 48. Kang, D. *et al.* DNA biomolecular-electronic encoder and decoder devices constructed by

522 multiplex biosensors. *NPG Asia Mater.* **4**, 1–6 (2012).

523 49. Sigen, A. *et al.* Hyperbranched PEG-based multi-NHS polymer and bioconjugation with
524 BSA. *Polym. Chem.* **8**, 1283–1287 (2017).

525 50. Thalla, P. K. *et al.* Chondroitin sulfate coatings display low platelet but high endothelial cell
526 adhesive properties favorable for vascular implants. *Biomacromolecules* **15**, 2512–2520
527 (2014).

528 51. Jonkheijm, P., Weinrich, D., Schröder, H., Niemeyer, C. M. & Waldmann, H. Chemical
529 strategies for generating protein biochips. *Angew. Chemie - Int. Ed.* **47**, 9618–9647 (2008).

530 52. Kwon, J. *et al.* Bright ligand-activatable fluorescent protein for high-quality multicolor live-
531 cell super-resolution microscopy. *Nat. Commun.* **11**, 1–11 (2020).

532 53. Liang, Q., Huang, Z., Zhang, Y. & Li, H. Immobilization of Ulp1 protease on NHS-activated
533 Sepharose: a useful tool for cleavage of the SUMO tag of recombinant proteins. *Biotechnol.*
534 *Lett.* **39**, 1025–1031 (2017).

535 54. Costa, S., Almeida, A., Castro, A. & Domingues, L. Fusion tags for protein solubility,
536 purification, and immunogenicity in Escherichia coli: The novel Fh8 system. *Front.*
537 *Microbiol.* **5**, 1–20 (2014).

538 55. Tanaka, T., Yamamoto, T., Tsukiji, S. & Nagamune, T. Site-specific protein modification on
539 living cells catalyzed by sortase. *ChemBioChem* **9**, 802–807 (2008).

540 56. Fernández-Suárez, M. *et al.* Redirecting lipoic acid ligase for cell surface protein labeling
541 with small-molecule probes. *Nat. Biotechnol.* **25**, 1483–1487 (2007).

542 57. Schumacher, D. *et al.* Versatile and Efficient Site-Specific Protein Functionalization by
543 Tubulin Tyrosine Ligase. *Angew. Chemie - Int. Ed.* **54**, 13787–13791 (2015).

544 58. Zucca, P., Fernandez-Lafuente, R. & Sanjust, E. Agarose and its derivatives as supports for
545 enzyme immobilization. *Molecules* **21**, 1–25 (2016).

546 59. Hwang, J. M. D., Piccinini, T. E., Lammel, C. J., Hadley, W. K. & Brooks, G. F. Effect of storage
547 temperature and pH on the stability of antimicrobial agents in MIC trays. *J. Clin. Microbiol.*
548 **23**, 959–961 (1986).

549 60. Gao, X. J., Chong, L. S., Kim, M. S. & Elowitz, M. B. Programmable protein circuits in living
550 cells. *Science (80-.).* **361**, 1252–1258 (2018).

551 61. Fink, T. *et al.* Design of fast proteolysis-based signaling and logic circuits in mammalian
552 cells. *Nat. Chem. Biol.* **15**, 115–122 (2019).

553 62. Gibson, D. G. *et al.* Enzymatic assembly of DNA molecules up to several hundred kilobases.
554 *Nat. Methods* **6**, 343–345 (2009).

555 63. Jumper, J. *et al.* Highly accurate protein structure prediction with AlphaFold. *Nature* **596**,
556 583–589 (2021).

557 64. Schrödinger, L. The PyMOL Molecular Graphics System. (2010).

558

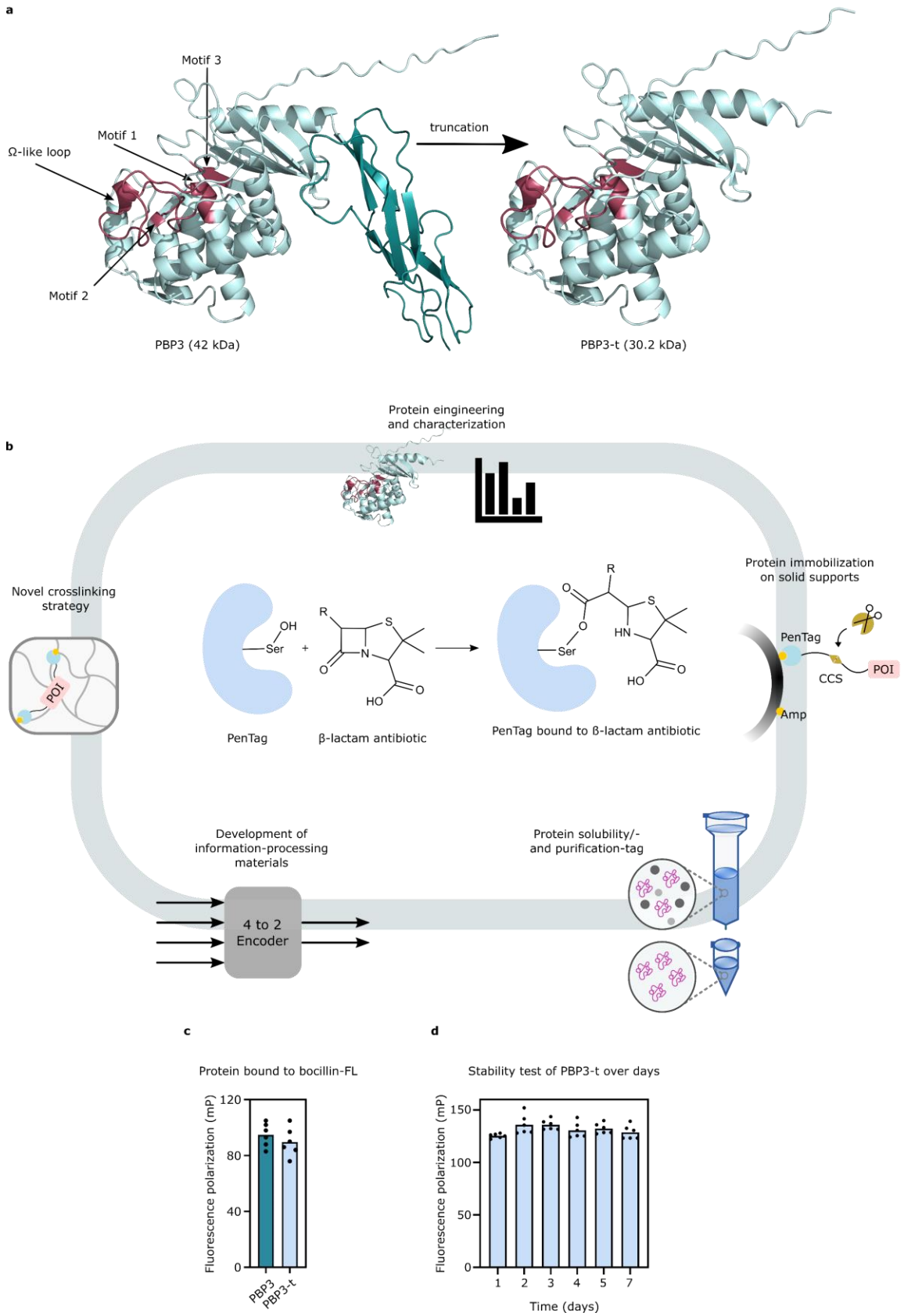

559 **Fig. 1| Engineering a new truncated version of PBP3. a**, Structure of full-length PBP3 (with

560 membrane anchor, left) and upon truncation (right). The membrane anchor is shown in dark cyan
561 and the rest of the protein shown in light cyan. In red, the active site of the protein consisting of
562 motif 1, 2, 3 and Ω-like loop is shown. Protein structure prediction is done by AlphaFold 2[63] and
563 figures are generated by PyMOL[64]. **b**, Mechanism of conjugation of ß-lactam antibiotics to PenTag
564 and an overview of applications that could benefit from this conjugation technique. **c,**
565 Fluorescence polarization measurements to compare the PBP3/bocillin-FL bond with PBP3-
566 t/bocillin-FL bond at RT. **d**, Fluorescence polarization of PBP3-t/bocillin-FL complex over several
567 days at 4 °C in PBS. Fluorescence polarization measurements consist of 3 separate replicates,
568 each measured twice and are shown as mean and indicating replicates.

569

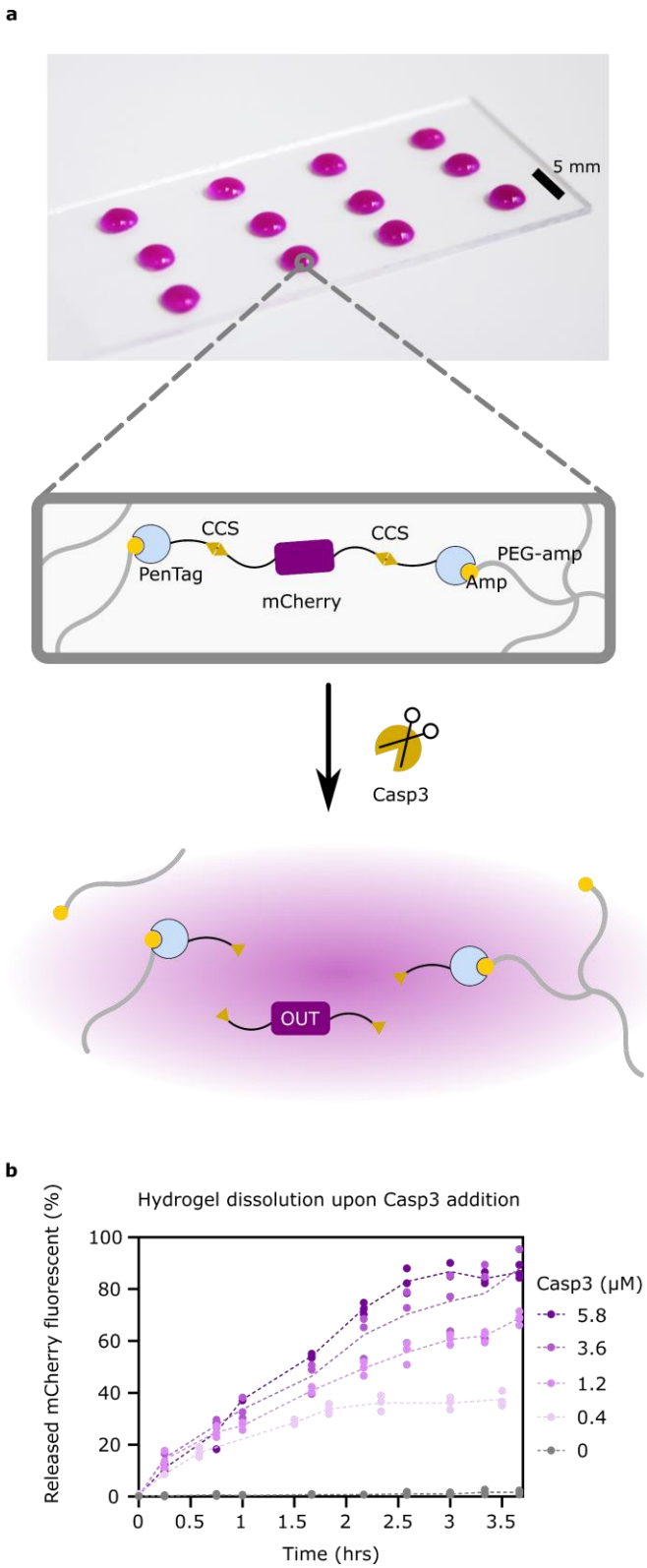

570 **Fig. 2| Synthesis of a stimuli-responsive hydrogel and its dissolution kinetics. a**, Picture of
571 synthesized hydrogels on a coated glass-slide and schematic of the building blocks involved in

572 crosslinking. **b**, Time-resolved dissolution of hydrogels upon addition of different Casp3 amounts.
573 Data represent 3-5 separate replicates for each condition, dotted lines connect the means of
574 each condition.

575

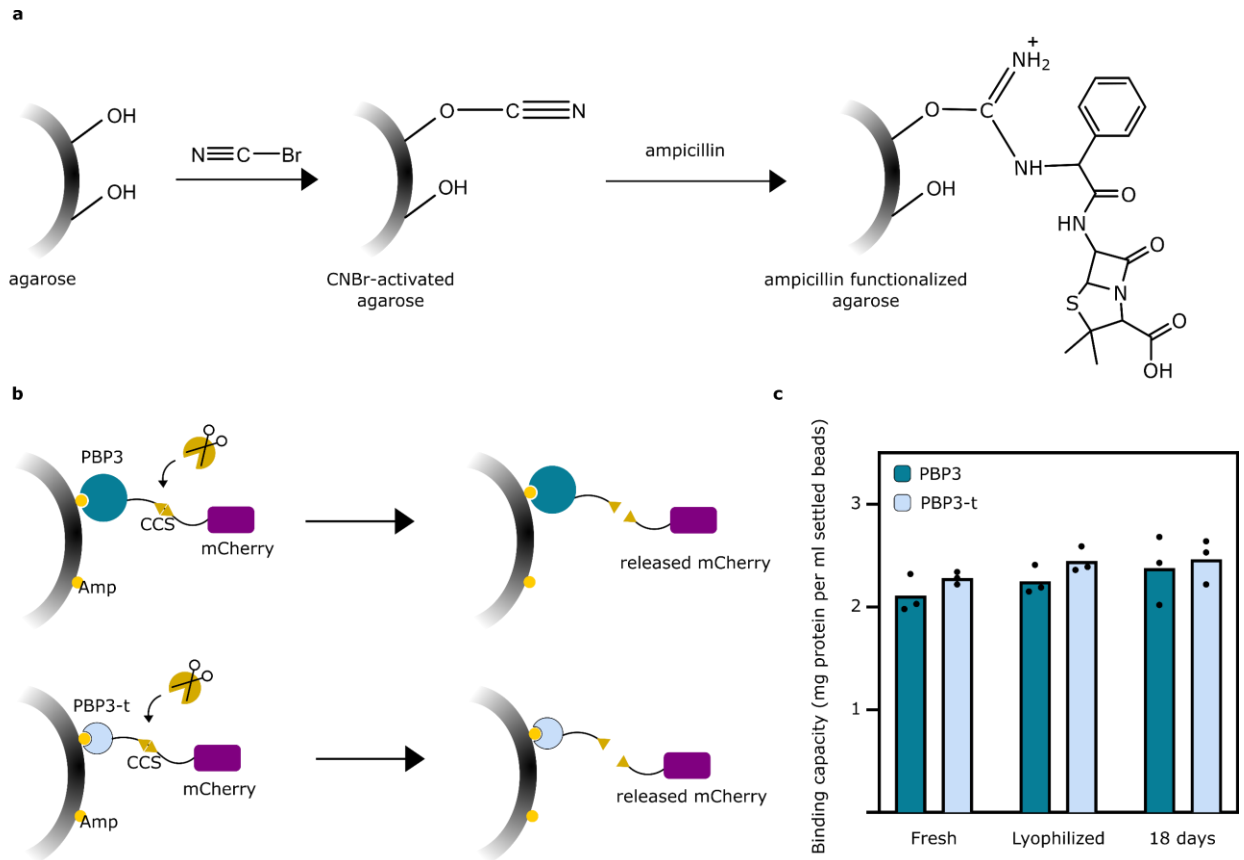

Fig. 3| Conjugation PenTagged proteins onto agarose beads. a, Functionalization of CNBr-activated agarose beads with ampicillin. **b**, Schematic representation of coupled PBP3-/or PBP3-t- fused mCherry on beads and mCherry release by adding Casp3 protease. **c**, mCherry release from ampicillin beads, captured by PenTag (either PBP3, or PBP3-t) at three different steps after functionalizing beads: right after functionalization, after lyophilization, and 18 days post-lyophilization. Binding capacity is reported as mg released protein per ml of settled beads. Bar charts represent the mean of 3 separate replicates.

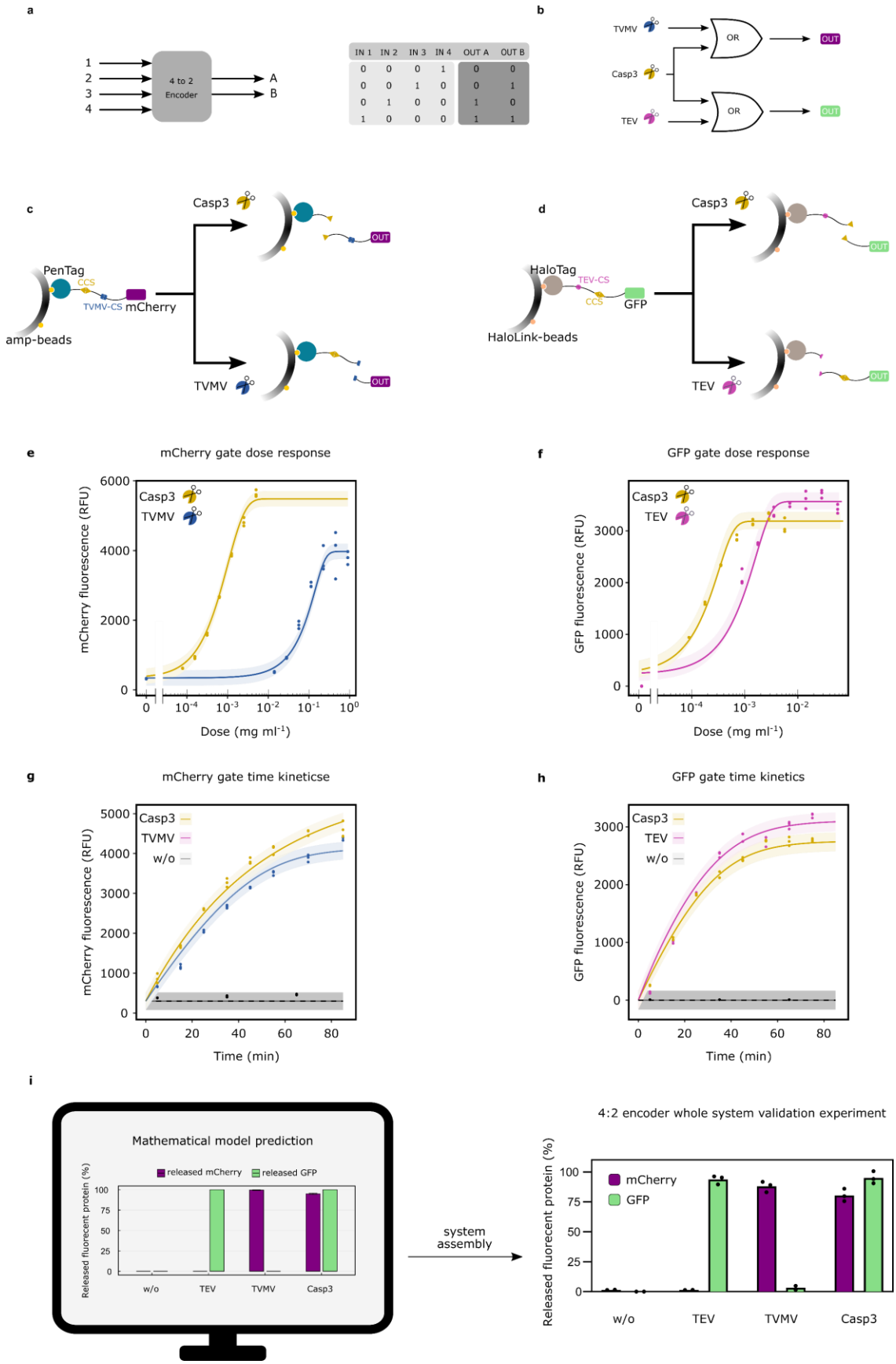

584 **Figure 4| Development of two orthogonal material-based OR gates and their combination in a**

585 **4:2 encoder set-up. a**, Schematic of a 4:2 encoder (left) and 4 different input/output
586 combinations of such a 4:2 encoder (right). **b**, Combination of two different OR gates sharing one
587 same input towards a 4:2 encoder. **c**, Schematic of mCherry OR gate. Output mCherry is supposed
588 to be released in presence of either Casp3, or TVMV protease, or both. Molecular design of
589 mCherry module consists of mCherry fused to PenTag by a linker containing cleavage sites for
590 Casp3 and TVMV. Protein is bound through PenTag on ampicillin functionalized crosslinked
591 agarose. **d**, Schematic of GFP OR gate. Output GFP is supposed to be released in presence of
592 either Casp3, or TEV protease, or both. Molecular design of GFP module, consisting of GFP fused
593 to HaloTag by a linker containing cleavage sites for TEV and Casp3. Output GFP is released in
594 presence of each of proteases. Protein is bound through HaloTag on HaloLink material. **e**, Data
595 and model fits of the dose-dependent release of mCherry from ampicillin material module upon
596 addition of different concentrations of TVMV and Casp3. **f**, Data and model fits of the dose-
597 dependent release of the GFP from HaloLink material module upon addition of different
598 concentrations of Casp3 and TEV. **g**, Data and model fits of the time-resolved measurements of
599 mCherry module upon addition of Casp3 or TVMV over time. **h**, Data and model fits of the time-
600 resolved measurements of GFP module upon addition of TEV or Casp3 over time. **i**, Combination
601 of both systems towards a 4:2 encoder system predicted by the mathematical model (left) and
602 validated by experiments (right). Triplicates were measured for the samples, and duplicates for
603 negative controls.